INDONESIAN JOURNAL ON GEOSCIENCE
Geological Agency
Ministry of Energy and Mineral Resources

Journal homepage: https://ijog.geologi.esdm.go.id
ISSN 2355-9314, e-ISSN 2355-9306

Gravity Data Analysis for Fault Identification and Earthquake Hypocentre Relocation Using Modified Joint Hypocentre Determination Method in Cianjur Area

Divia Isyania Putri[1], Suwondo[1], Mohammad Iqbal Tawakal[2], Tati Zera[1], and Sutrisno[1]

[1]Department of Physics, UIN Syarif Hidayatullah Jakarta, Banten 15412, Indonesia
[2]Balai Besar Meteorologi, Klimatologi, dan Geofisika Wilayah II

Corresponding author: suwondo@uinjkt.ac.id
Manuscript received: March, 01, 2024; revised: February, 10, 2025;
approved: February, 16, 2026; available online: July, 24, 2026

Abstract - An earthquake with a magnitude of M 5.6 occurred in Cianjur, West Java, on November 21st, 2022, and left 321 people dead. This event raised concerns about the potential for aftershocks, necessitating an in-depth analysis to evaluate future seismic risk in Cianjur. This study aims to identify the type of fault that triggered the earthquake and to relocate the hypocentre in the Cianjur area. First horizontal derivative (FHD) and second vertical derivative (SVD) methods from gravity data were used for mapping the fault structure and the fault type. Fault location is represented by zero SVD and peak FHD to determine the type of fault; the maximum FHD and minimum SVD values were compared. The correlation results of FHD and SVD graphs obtained a fault line with a northwest to southeast direction on the Cugenang Fault and Cimandiri Fault line, with its movement direction from Pelabuhan Ratu with a shear fault type. The results of the relocation analysis show the existence of two identified alignment structures in the direction of north northeast–south southeast (NNW–SSE) and east northeast to west-southwest (WSW-ENE) which form a group on the trendline of the fault zone, as evidenced by the tectonic activity in the Cianjur area caused by the existence of a pair of mutually perpendicular horizontal faults (shear conjugate faults).

Keywords: earthquake, FHD (First Horizontal Derivative), SVD (Second Vertical Derivative), shear fault, earthquake relocation, Cianjur Earthquake November 21st 2022

How to cite this article:
Putri, D.I., Suwondo, Tawakal, M.I., Zera, T., and Sutrisno, 2026. Gravity Data Analysis for Fault Identification and Earthquake Hypocentre Relocation Using Modified Joint Hypocentre Determination Method in Cianjur Area. *Indonesian Journal on Geoscience*, 13 (2), p.297-312. DOI:10.17014/ ijog.13.2.297-312

Introduction

Background

An earthquake is a phenomenon in which a jolt or shock originates from within the earth and then propagates to the earth's surface. Earthquakes occur as a result of a sudden release of energy, which produces particle vibrations that spread in all directions due to the subduction process. Earthquakes occur due to the rupture or shifting of rocks within the Earth's crust. These vibrations then travel through the ground in the form of vibrational waves, and humans on the surface of the Earth feel the vibrations, which eventually become known as 'earthquakes'.

One of the earthquakes that recently struck Indonesia was the earthquake that occurred in Cianjur region on November 21st, 2022. This earthquake was categorized as a shallow crustal earthquake and had a mainshock-aftershocks type pattern, *i.e.,* a main earthquake followed by a series of aftershocks. Based on Supendi *et* *al.* (2022), the Cianjur region is traversed by the Cimandiri Fault of the Rajamandala segment, which has a left-lateral strike-slip mechanism, making the area vulnerable to earthquake threats. The Cimandiri Fault stretches from Pelabuhan Ratu Bay in Sukabumi to Padalarang in West Bandung Regency, with a total length of about 100 km. The fault is divided into three segments, namely, the Cimandiri Segment (with a fault mechanism), the Nyalindung-Cibeber Segment (with a fault mechanism), and the Rajamandala Segment. However, recent research (Supendi *et al*., 2023) shows that the 2022 Cianjur earthquake did not originate from the Cimandiri Fault but rather from a local fault structure in the Cugenang area. This finding has become the main focus of this study. The Cianjur earthquake is associated with the Cimandiri Fault, which, originating from a local fault structure referred to as the Cugenang Fault, which plays an important role in controlling the seismic activity in the region.

One of the relevant geophysical methods in fault research is the gravity method, because it is able to produce a picture of density distribution in the subsurface layer. Subsurface geological structures can be recognized using the gravity method, which is a passive geophysical method. Variations in the earth's gravity field occur due to differences in density or mass density between rocks in the subsurface. These differences in density values make it possible to identify anomalies related to geological structures, such as the presence of faults. In this research, three types of gravity satellite data variations were taken, namely topographic data, geoid data, and gravity disturbance data. In addition to the gravity method, this study uses the modified joint hypocentre determination (MJHD) method using Velest 3.3 software because the method limits the depth and the epicentre of the earthquake. With this approach, even when faced with different variations in earth structure and non-uniform station placement, the method is still able to identify locations with a significant degree of accuracy. It also has the ability to process a large amount of data simultaneously and make adjustments to the stations used so that a clearer picture of tectonic and subduction patterns can be presented.

Geological Overview

Java is one of the regions in Indonesia with a very high population and infrastructure density. The risk of earthquake hazards in this region is strongly influenced by the population and the presence of infrastructure in areas that have been identified as disaster-prone. Below is a geological map of the Cianjur region. As one of the regions in Java, the geology of West Java is unique. Geological activities that last for millions of years have produced various types of rocks, including sedimentary rocks, igneous rocks (both extrusive and intrusive), and metamorphic rocks with varying age ranges.

The researched area is located in Cianjur Regency, precisely around the Cugenang Fault (Figure 1). The figure in the purple line box shows the line of the Cugenang Fault, which is perpendicular to the location of the main earthquake in Cianjur (Figure 1). The earthquake data used was obtained from BMKG. Meanwhile, data related to the Cimandiri Fault used SHP files obtained from the map of seismic sources and earthquake hazard in Indonesia (PUSGEN, 2017). The delineation of the Cugenang Fault in this study is the result of gravity analysis (FHD and SVD), which was then compared with the findings of Supendi *et al*. (2023), who also reported the fault activity in Cugenang.

The geological structure in West Java is largely influenced by the collision interaction between the Indo-Australian Plate, which subducts beneath the Eurasian Plate. This plate collision activity forms the main tectonic elements in West Java, such as troughs, nonvolcanic outer arcs, fore-arc basins, magmatism pathways, back-arc basins, and the Sunda Shelf. This tectonic interaction has formed the major tectonic framework of West Java. Within this regional setting, the Cianjur area is characterized by complex geological structures related to active tectonic processes. In addition to the regionally scaled Cimandiri structure, recent

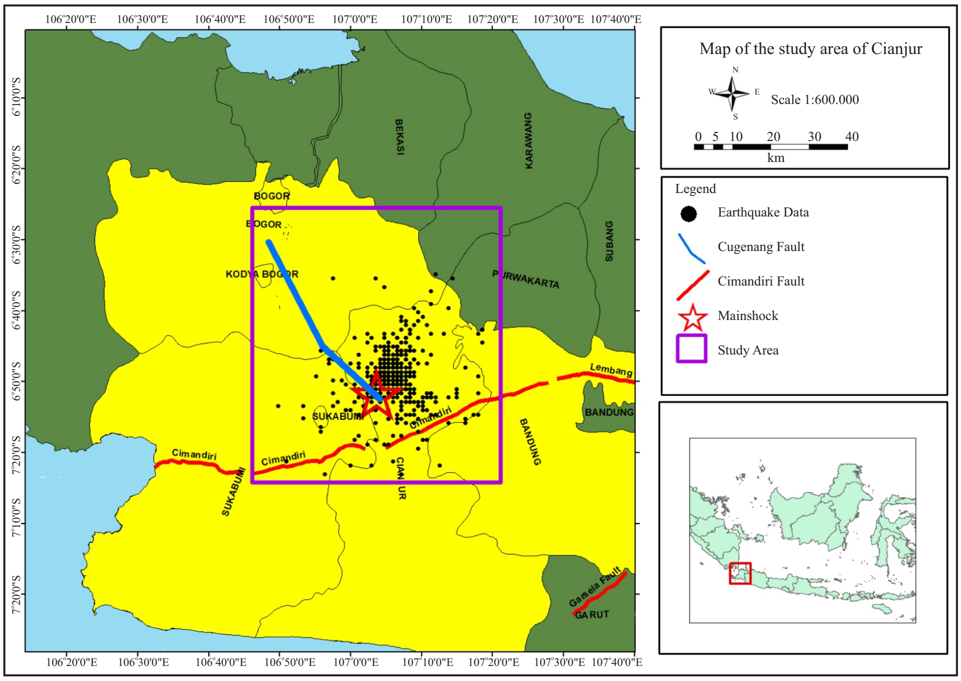

Figure 1. The studied area in Cianjur is shown by the purple line box.

seismotectonic data also indicate the presence of an active fault in Cugenang that is associated with the 2022 earthquake.

The lithologic geology of Cianjur and Sukabumi is based on Figure 2 of the regional geologic map, which includes

1. The Qv Formation, the result of active volcanic deposits consisting of a mixture of lava, breccia, tuff, and lava deposits that are generally composed of andesite to basalt, formed in the Holocene era and was deposited on top of the underlying formations with no parallel.
2. The Qpv Formation, consisting of volcanic spice composed of andesite-basalt sourced from an old volcano of Pleistocene age.
3. The Tnv Formation consists of andesitic breccia, basalt, lava, tuffaceous sandstone, and conglomerate of Neogene in age.
4. The Tmss Formation, consisting of sandstone, sandstone tuff, claystone, tuff, and mudstone interbedded with conglomerate of various materials, marl, and limestone, with submarine inserts of Middle Miocene age.
5. The Tomss Formation consists of marl, claystone, sandstone, tuff, and limestone lenses.
6. The Tmi formation, consisting of granite, granodiorite, diorite, dacite, and quartz diorite, is of Miocene age.
7. The Tlss formation consists of breccia of various materials, tuff, sandstone, conglomerate of various materials, lava, eroded wood, altered rock, and claystone of early Miocene age.
8. The Tlls Formation, consisting of limestone, marl, sandstone, claystone. The Tlls Formation is of Early Miocene age.
9. The Tmvs formation consists of volcanic breccia, tuff, lava, andesite, basalt, and eroded wood of Late Miocene age.
10. The Tmib Formation, consists of breakthrough rocks generally composed of medium plagioclase and hornblende andesite around Mount Sanggabuana and Mount Parang.

Methods

The research used two methods, namely the gravity method to identify faults and the modified joint hypocentre determination method for earthquake hypocentre relocation. The following are the data processing stages of the two methods:

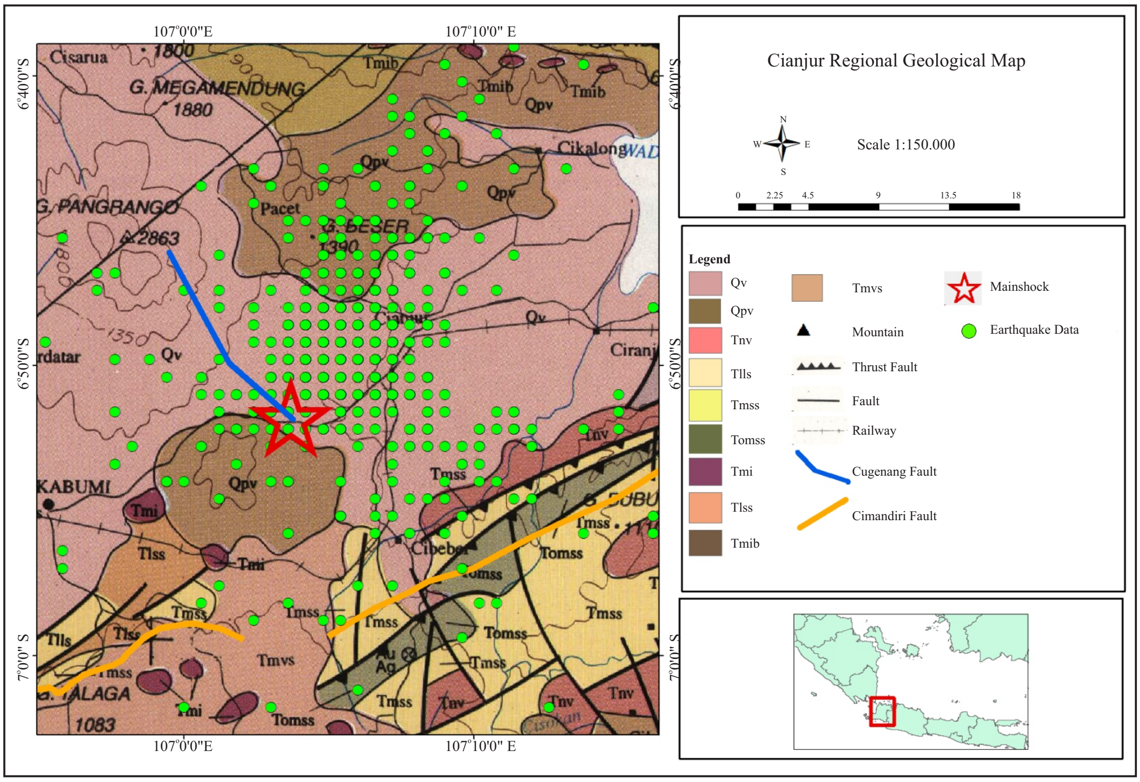

Figure 2. Regional geologic map of Cianjur area (Sudjatmiko, 1972).

Gravity Method

In the gravity method, there are topographic, geoid, and gravity disturbance data. The data were quoted from the icgem.potsdam website and converted to the UTM zone according to the researched area, namely the UTM 48S zone, with surfer software. Then calculated with Microsoft Excel to obtain the CBA (Complete Bouguer Anomaly) value, local and regional boundaries.

The gravity method uses Newton's principle of gravity 1. This principle states that when two bodies with masses m_1 and m_2 are separated by a distance R, they will attract each other with a force proportional to the mass of each body and inversely proportional to the distance R. Newton's law can be formulated in the following equation:

$$F = G\frac{(m_1 m_2)}{r^2} \quad \text{...} \quad (1)$$

where:

F = gravitational force (N)

G = gravitational constant (9,83 m/s^2)

m_1 = mass of the pendulum in the device (kg)

m_2 = mass below the surface (kg)

r^2 = distance (m)

Gravity field anomalies refer to the difference between the measured gravity field value at a particular location or position (x, y, z) and the theoretical gravity field value expected at the same location. These gravitational field differences are caused by variations in the density of the earth's subsurface. Data processing using the gravity method carried out three corrections, namely free air correction, Bouger correction, and terrain correction. The three data are further processed using Oasis Montaj software and produce regional anomaly, residual anomaly, FHD (first horizontal derivative), and SVD (second vertical derivative) modeling. The following is the equation formulation of the three gravity corrections: It should be noted that gravity-based fault interpretations are indirect. Therefore, these identification results need to be validated with surface geological data or geomorphological analysis.

a. Free Air Correction

Gravitational acceleration attracts objects on earth, and free air correction (FAC) is used to improve measurement accuracy. This correction is only necessary when measurements are taken at locations above or below the geoid, *i.e.* sea level:

$$g_{fA} = 0.3086 \text{ x } h \quad (2)$$

Description:

g_{fA} = free air correction (mgal)

h = height of the point above sea level (m)

b. Terrain Correction

Topographic correction is required to overcome the effects of irregular mass distribution around the measurement site. In the Bouguer correction method, it is assumed that the measurement point is on a very flat and wide surface:

$$\delta g_T = \gamma\rho\theta(r_2 - r_1) + \sqrt{r_1^2 + z^2} - \sqrt{r_2^2 + z^2} \quad (3)$$

where:

δg_t = terrain correction (mgal)

γ = universal gravitational constant

Δ = compartment elevation difference (m)

r_1 = radius of inner compartment (m)

r_2 = radius of outer compartment (m)

θ = angle formed by the compartments (degree)

c. *Bouger Correction*

The Bouguer correction considers the amount of mass between the measurement station and the geoid plane. This process involves calculating the gravitational attraction force arising from the rock, which is a slab layer with thickness H and average density of ρ.

$$\delta g_b = 2\Pi G ph \quad (4)$$

where:

β = $2^{\Pi}G = 0{,}4192.u.m^2 Mg^{-1}$

G = $6{,}67 \text{ x } 10^{-8} m^3 Mg^{-1} S^{-2}$

ρ = rock density (gram/cm^3)

h = altitude (m)

To determine the type of fault in the researched area, the fault data in SHP format was imported, then a section was traversed three times from west to east for the Cugenang Fault research area and a section three times from north to south for The Cimandiri Fault research area.

This method uses the WHU-SWPU-GOGR2022S, 2023 model with a 0.01 km grid of gravity satellite data (icgem.postdam) aiming to obtain high spatial resolution. With a fine grid, information about gravity anomalies on the earth surface can be obtained in greater detail, making it possible to identify subsurface structures more accurately. High spatial resolution also makes it possible to detect small anomalies that may have geological or geophysical significance. Therefore, the use of 0.01 km grids in gravity data methods is essential for applications that require high detail in subsurface modeling and analysis. There are three types of data obtained from the website, namely, topographic data, gravity disturbance data, and geoid data. Each of the three data points was corrected using gravity correction.

Modified Joint Hypocentre Determinaton Method

In this method, the data is obtained from the BMKG catalogue, namely earthquake data for 549 earthquake events in the period of November 11th to June 11th, 2023, and station data for 116 station points. Both data were filtered to determine the closest earthquake point to the main earthquake. Then, it is processed further using Velest software.

The joint hypocentre determination (JHD) method, first coined by Douglas in 1967 and developed by Hurukawa and Imoto in 1992, can provide highly accurate estimates of earthquake locations. Although the earth structure is not uniform and the distribution of stations is uneven, accurate results can still be achieved. Thanks to the application of restrictions on depth and epicentre.

The principle of the MJHD method involves the simultaneous processing of earthquake travel times to improve the accuracy of hypocentre location estimation. By integrating station adjustments in the form of azimuth factors and relative station distances, the precision of the results can be improved, even if the velocity model applied is the same as that used to determine the hypocenter. The MJHD method can be formulated in the following equation:

$$(O-C)_{ij} = \left(t_{ij} - TO_j\right) - T_{ij}, \\ = \frac{\partial t_{ij}}{\partial x_i}\partial x_j + \frac{\partial t_{ij}}{\partial y_i} + \partial y_j + \frac{\partial t_{ij}}{\partial z_i} + dTO_j + dS_i \quad \text{......... (5)}$$

where:

$(O\text{-}C)_{ij}$ = residual travel time at earthquake i at station j

O = observed travel time (seconds)

C = calculated travel time (seconds)

t_{ij} = arrival time of earthquake j at station i

T_{ij} = travel time of earthquake j at station i

dS_i = correction for station i

dTO_j = trial hypocentre correction of the j event

$\partial x,y,z$ = trial hypocentre correction of event j

TO_j = earthquake time (seconds)

a. Data Selection

Figure 3 is the earthquake input data. The first step, selection input data based on the researched area. Data research using 116 stations and 549 earthquake data.

b. Data Processing using Velest 3.3 Software

Data processing using Velest 3.3 software requires several inputs with the following file extensions:

1) *.cmn is the file extension for control parameters.
2) *.sta is the file extension for the station list
3) *.cnv is a file extension for earthquake data 3) After the input data was processed, the resulting output data was in the form of the final relocation of the hypocentre, latitude, longitude, depth and magnitude with new files, namely:
4) *.out (main printout)

Figure 4 is the station input data used in Velest 3.3 software; data writing must be in accordance with the format used by Velest 3.3 software.

Result

Analysis of FHD Map from Gravity Data

The FHD map derived from the CBA map can be derived vertically (FHD Y) and also horizontally (FHD X), which is used to identify the fault as FHD Z (resultant between FHD X and FHD

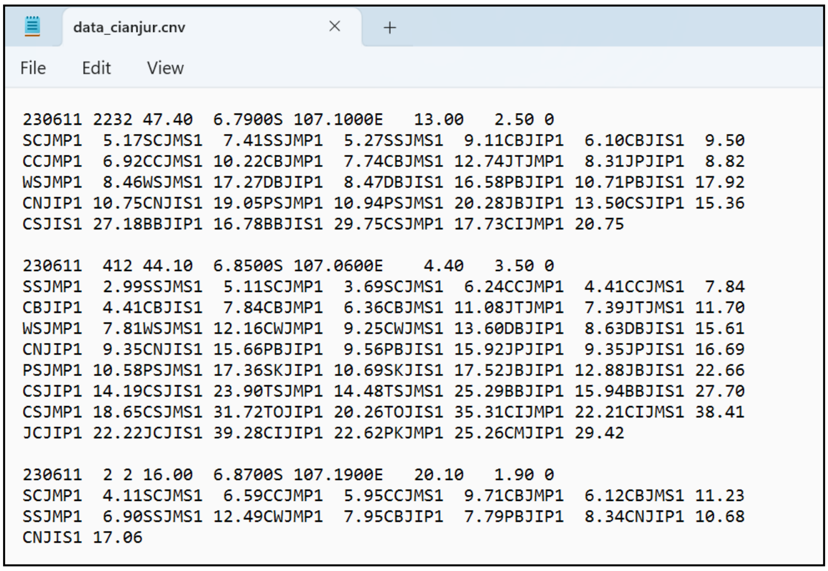

```
data_cianjur.cnv
File    Edit    View

230611 2232 47.40  6.7900S 107.1000E   13.00   2.50 0
SCJMP1  5.17SCJMS1  7.41SSJMP1  5.27SSJMS1  9.11CBJIP1  6.10CBJIS1  9.50
CCJMP1  6.92CCJMS1 10.22CBJMP1  7.74CBJMS1 12.74JTJMP1  8.31JPJIP1  8.82
WSJMP1  8.46WSJMS1 17.27DBJIP1  8.47DBJIS1 16.58PBJIP1 10.71PBJIS1 17.92
CNJIP1 10.75CNJIS1 19.05PSJMP1 10.94PSJMS1 20.28JBJIP1 13.50CSJIP1 15.36
CSJIS1 27.18BBJIP1 16.78BBJIS1 29.75CSJMP1 17.73CIJMP1 20.75

230611  412 44.10  6.8500S 107.0600E    4.40   3.50 0
SSJMP1  2.99SSJMS1  5.11SCJMP1  3.69SCJMS1  6.24CCJMP1  4.41CCJMS1  7.84
CBJIP1  4.41CBJIS1  7.84CBJMP1  6.36CBJMS1 11.08JTJMP1  7.39JTJMS1 11.70
WSJMP1  7.81WSJMS1 12.16CWJMP1  9.25CWJMS1 13.60DBJIP1  8.63DBJIS1 15.61
CNJIP1  9.35CNJIS1 15.66PBJIP1  9.56PBJIS1 15.92JPJIP1  9.35JPJIS1 16.69
PSJMP1 10.58PSJMS1 17.36SKJIP1 10.69SKJIS1 17.52JBJIP1 12.88JBJIS1 22.66
CSJIP1 14.19CSJIS1 23.90TSJMP1 14.48TSJMS1 25.29BBJIP1 15.94BBJIS1 27.70
CSJMP1 18.65CSJMS1 31.72TOJIP1 20.26TOJIS1 35.31CIJMP1 22.21CIJMS1 38.41
JCJIP1 22.22JCJIS1 39.28CIJIP1 22.62PKJMP1 25.26CMJIP1 29.42

230611  2 2 16.00  6.8700S 107.1900E   20.10   1.90 0
SCJMP1  4.11SCJMS1  6.59CCJMP1  5.95CCJMS1  9.71CBJMP1  6.12CBJMS1 11.23
SSJMP1  6.90SSJMS1 12.49CWJMP1  7.95CBJIP1  7.79PBJIP1  8.34CNJIP1 10.68
CNJIS1 17.06
```

Figure 3. Earthquake input data.

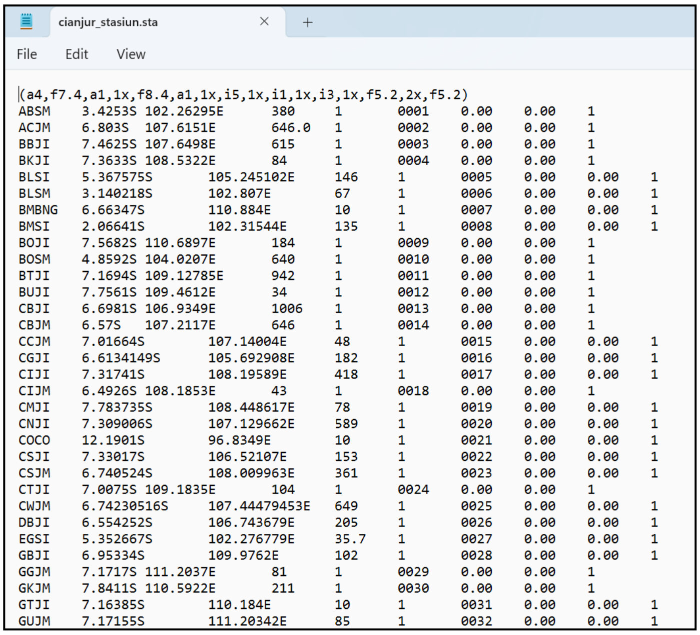


```
(a4,f7.4,a1,1x,f8.4,a1,1x,i5,1x,i1,1x,i3,1x,f5.2,2x,f5.2)
ABSM    3.4253S 102.26295E      380     1       0001    0.00    0.00    1
ACJM    6.803S  107.6151E       646.0   1       0002    0.00    0.00    1
BBJI    7.4625S 107.6498E       615     1       0003    0.00    0.00    1
BKJI    7.3633S 108.5322E       84      1       0004    0.00    0.00    1
BLSI    5.367575S       105.245102E     146     1       0005    0.00    0.00    1
BLSM    3.140218S       102.807E        67      1       0006    0.00    0.00    1
BMBNG   6.66347S        110.884E        10      1       0007    0.00    0.00    1
BMSI    2.06641S        102.31544E      135     1       0008    0.00    0.00    1
BOJI    7.5682S 110.6897E       184     1       0009    0.00    0.00    1
BOSM    4.8592S 104.0207E       640     1       0010    0.00    0.00    1
BTJI    7.1694S 109.12785E      942     1       0011    0.00    0.00    1
BUJI    7.7561S 109.4612E       34      1       0012    0.00    0.00    1
CBJI    6.6981S 106.9349E       1006    1       0013    0.00    0.00    1
CBJM    6.57S   107.2117E       646     1       0014    0.00    0.00    1
CCJM    7.01664S        107.14004E      48      1       0015    0.00    0.00    1
CGJI    6.6134149S      105.692908E     182     1       0016    0.00    0.00    1
CIJI    7.31741S        108.19589E      418     1       0017    0.00    0.00    1
CIJM    6.4926S 108.1853E       43      1       0018    0.00    0.00    1
CMJI    7.783735S       108.448617E     78      1       0019    0.00    0.00    1
CNJI    7.309006S       107.129662E     589     1       0020    0.00    0.00    1
COCO    12.1901S        96.8349E        10      1       0021    0.00    0.00    1
CSJI    7.33017S        106.52107E      153     1       0022    0.00    0.00    1
CSJM    6.740524S       108.009963E     361     1       0023    0.00    0.00    1
CTJI    7.0075S 109.1835E       104     1       0024    0.00    0.00    1
CWJM    6.74230516S     107.44479453E   649     1       0025    0.00    0.00    1
DBJI    6.554252S       106.743679E     205     1       0026    0.00    0.00    1
EGSI    5.352667S       102.276779E     35.7    1       0027    0.00    0.00    1
GBJI    6.95334S        109.9762E       102     1       0028    0.00    0.00    1
GGJM    7.1717S 111.2037E       81      1       0029    0.00    0.00    1
GKJM    7.8411S 110.5922E       211     1       0030    0.00    0.00    1
GTJI    7.16385S        110.184E        10      1       0031    0.00    0.00    1
GUJM    7.17155S        111.20342E      85      1       0032    0.00    0.00    1
```

Figure 4. Station input data.

Y). FHD analysis aims to find the limit of density contrast from the heavy force data characterized by high values. If the FHD is low, then it indicates that the zone is stable by conducting three sections in the west to east direction for the Cugenang Fault and three sections in the north to south direction for the Cimandiri Fault that cuts the researched area.

The characteristics of the FHD method indicate the presence of a fault, which can be observed from either the minimum or maximum peak. Based on the FHD map in Figure 5, the gravity value ranges from 0.0004784 to 0.0185868 mgal, with high anomalies dominated by basalt rocks and low anomalies associated with coal. In Figure 5, it can be seen that there is a Cugenang Fault that runs between the slicing points described above. This Cugenang Fault refers to the main earthquake point (star symbol). This anomaly pattern is not associated with the Cimandiri Fault but rather indicates the presence of a local structure in Cugenang that acts as the earthquake source.

Analysis of Second Vertical Derivative (SVD) Map from Gravity Data

SVD analysis was used to identify fault types by deriving the CBA values with respect to the z-axis at second order. This method aims to focus the data on the zero anomalies stored in the gravity data, as values of 0 mgal/m² can indicate the presence of lateral density contrasts characterized as maximum and minimum values, indicating the presence of structural plane boundaries (Figure 6).

Discussion

Analysis Results of Cugenang Fault and Cimandiri Fault Types

The initial process of fault type analysis is the correlation of the FHD and SVD graphs by digitizing the FHD and SVD grids vertically (Y) and horizontally (X) according to the direction of the digitization. If the peak of the FHD graph and the 0 point of the SVD graph are found at the same point, a fault can be suspected at that location. These two graphs will confirm the location of the fault. This graph is based on a line perpendicular to the fault. In this graph, the x-axis is the coordinate location on UTM Y or UTM X according to the direction of digitization, while the y-axis is the normalized SVD and FHD values. The values in each graph are normalized to

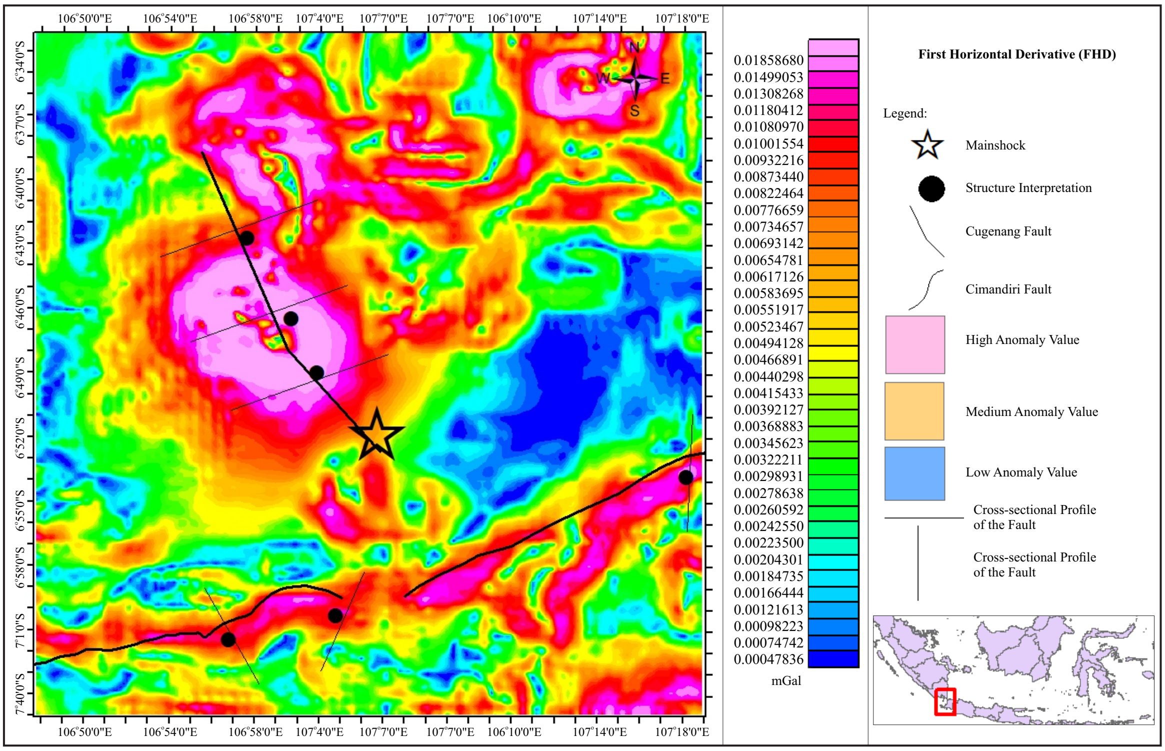

Figure 5. FHD (First Horizontal Derrivative) map modeling.

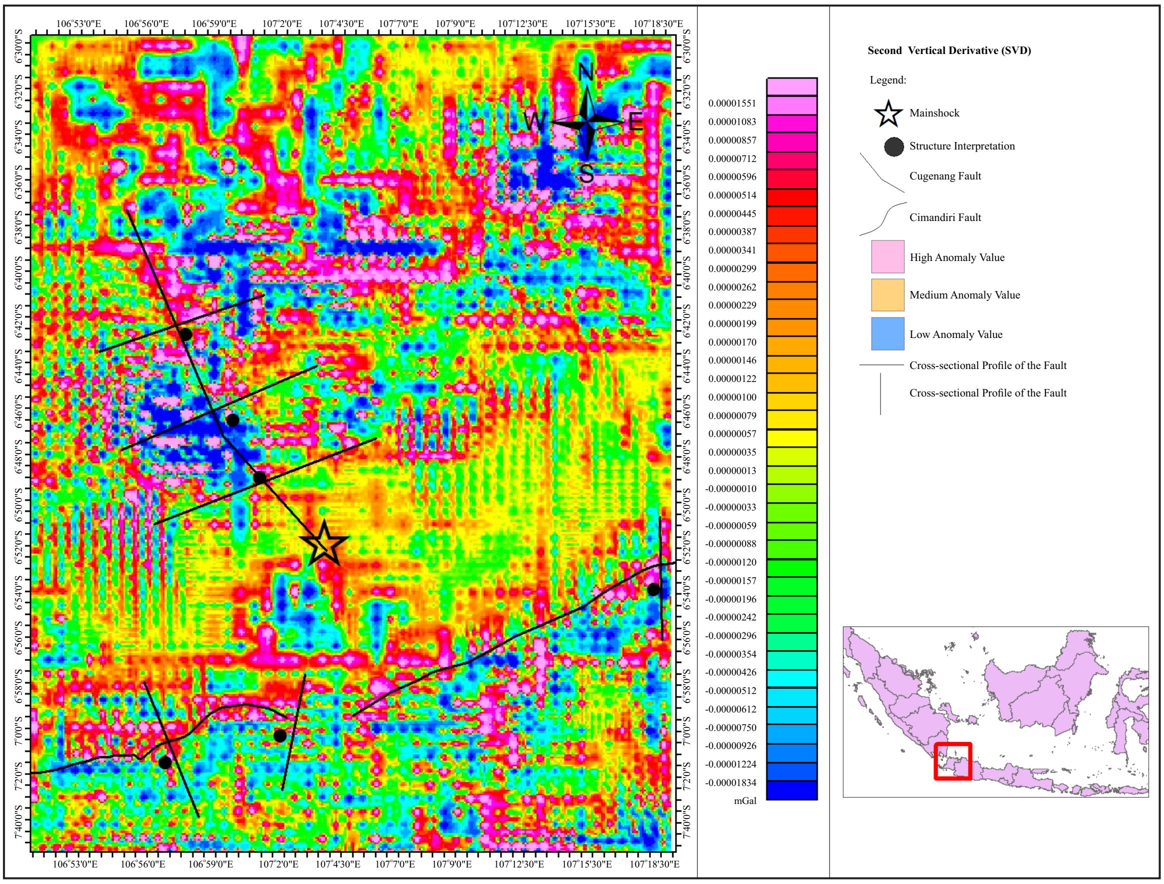

Figure 6. SVD (Second Vertical Derrivative) map modeling.

make it easier to read. Normalization was done by dividing all values by the overall maximum value of each absolute value on the graph.

Figures 7a–c present the FHD and SVD slices across the Cugenang Fault, respectively, illustrating the spatial variations in the studied parameters and their correlation with the fault geometry. Based on the interpretation results in Figure 8, it can be represented in Table 1. Based on the image in section 1, incision A - A' has the same value between SVD Min and SVD Max, which is 0.3. While section 2 in section B - B' has the same value between SVD Min and SVD Max, which is 0.03. And section 3 at section C - C' has the same value between SVD Min and SVD Max, which is 0.09. Therefore, the fault segments at incision A-A', B- B', and C-C' can be classified as strike-slip faults.

Showing slicing that fault-type analysis is necessary because the Cianjur earthquake was caused by active fault movement. Gravity analysis shows differences in rock density along the fault line, indicating subsurface tectonic activity. Regionally, Cianjur is in a zone influenced by the tectonic dynamics of the Cimandiri Fault and the subduction activity of the Indo-Australian Plate against the Eurasian Plate, which can trigger the movement of local faults, including the Cugenang Fault. The Cugenang Fault is a newly identified fault in Cianjur. This fault stretches for approximately 9 km, making it prone to causing earthquakes in the area. The correlation analysis results of the FHD and SVD graphs of the Cugenang Fault indicate a shear fault. According to BMKG research conducted by Supendi *et al.* (2023) (Figure 8), the focal mechanism of the main earthquake with a

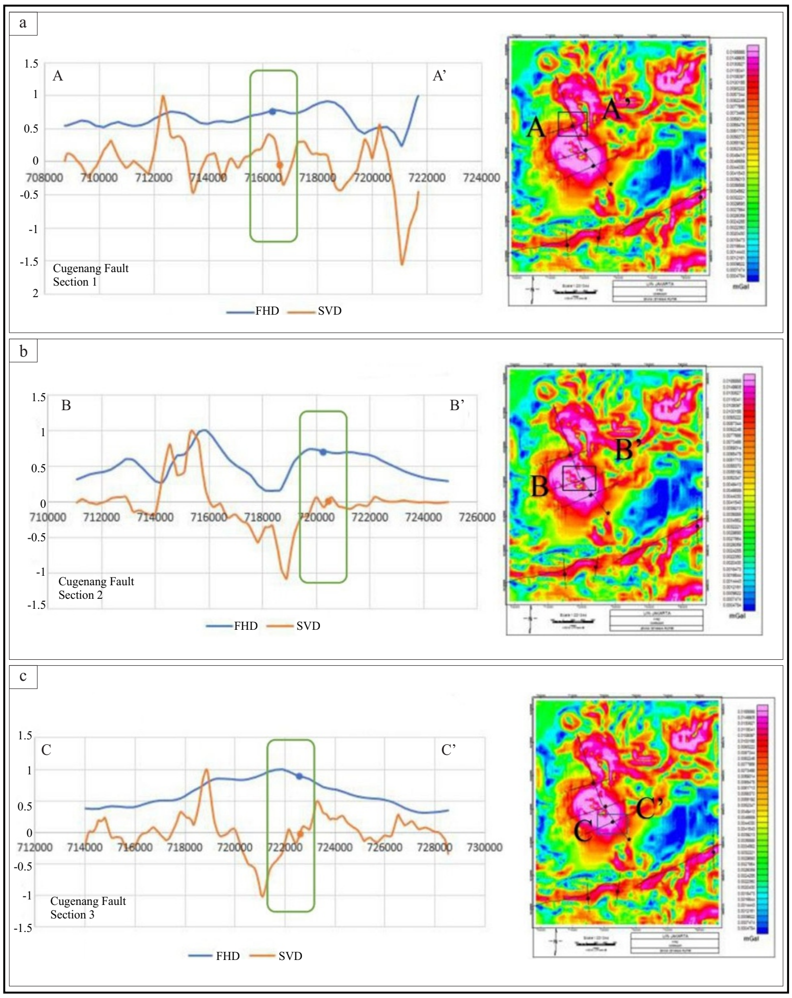

Figure 7. Slicing of FHD and SVD gravity through Cugenang Fault (box symbol).

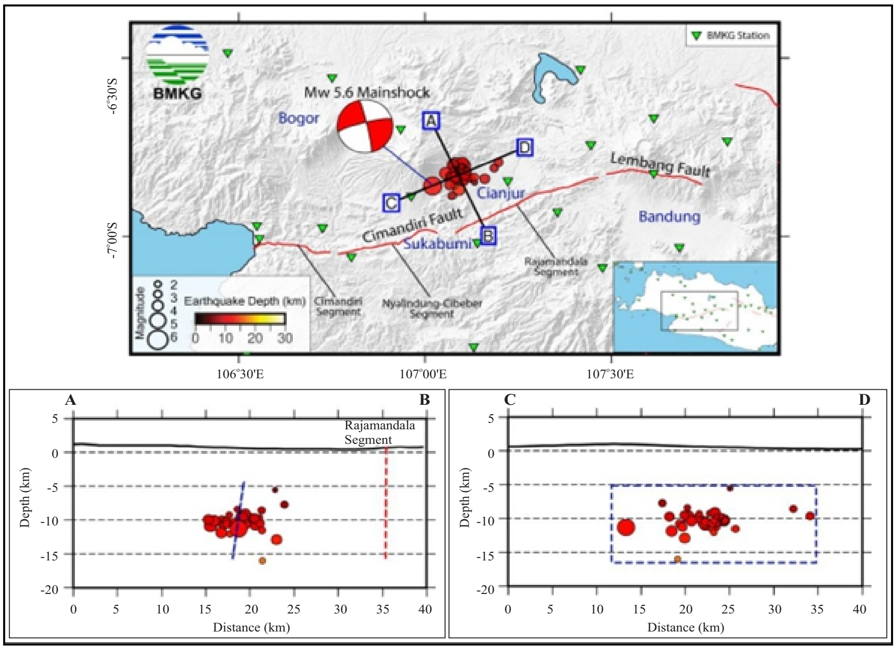

Figure 8. The epicentre and hypocentre of the Cianjur earthquake were relocated on November 21st, 2022 (BMKG) (Supendi *et al*., 2022).

Table 1. Interpretation of Cugenang Fault Type Based on Section 1 to Section 3

Cugenang			
Fault	**SVD *max***	**SVD min**	**Type**
Slicing 1	0.3	0.3	Strike Slip Fault
Slicing 2	0.03	0.03	Strike Slip Fault
Slicing 3	0.09	0.09	Strike Slip Fault

magnitude of Mw 5.6 indicates a sinistral strike-slip fault with a southwest-northeast orientation. This movement pattern is similar to the dominant movement that occurs on the Cimandiri Fault of the Rajamandala segment.

The fault analysis is shown in Figures 9a-c, used to determine the type of the Cimandiri Fault, because the Cimandiri Fault is an active shear fault approximately 100 km long, located in West Java. This fault is often cited as the trigger for many large earthquakes in the region. The Cimandiri Fault triggers earthquakes in Cianjur due to its active nature, which causes movement and shifting in the zone.

According to the interpretation results presented in Figure 9, Table 2, section 1, indicates that incision A - A' exhibits identical values for SVD Min and SVD Max, both measuring 0.5. In Section B, subsection B', the value between SVD Min and SVD Max is 0.8. Section 3 at section C - C' has an identical value of 0.3 between SVD Min and SVD Max. The correlation analysis of the FHD and SVD graphs for the Cimandiri Fault indicates the presence of a shear fault. This analysis indicates that the fault segments at incisions A-A', B-B', and C-C' can be categorised as strike-slip faults, consistent with the findings of Supendi *et al*., 2023.

Results of Relocation of Earthquake Hypocentre by Modified Joint Hypocentre Determination Method

The subsurface layer of the earth through which earthquake waves travel exhibits a wide variety of properties. This variability is the cause of differences in the determination of hypocentre locations by different stations, resulting in the distribution and recording of different events (Guci *et al*., 2020). Therefore, further research is needed to reduce possible errors caused by inac-

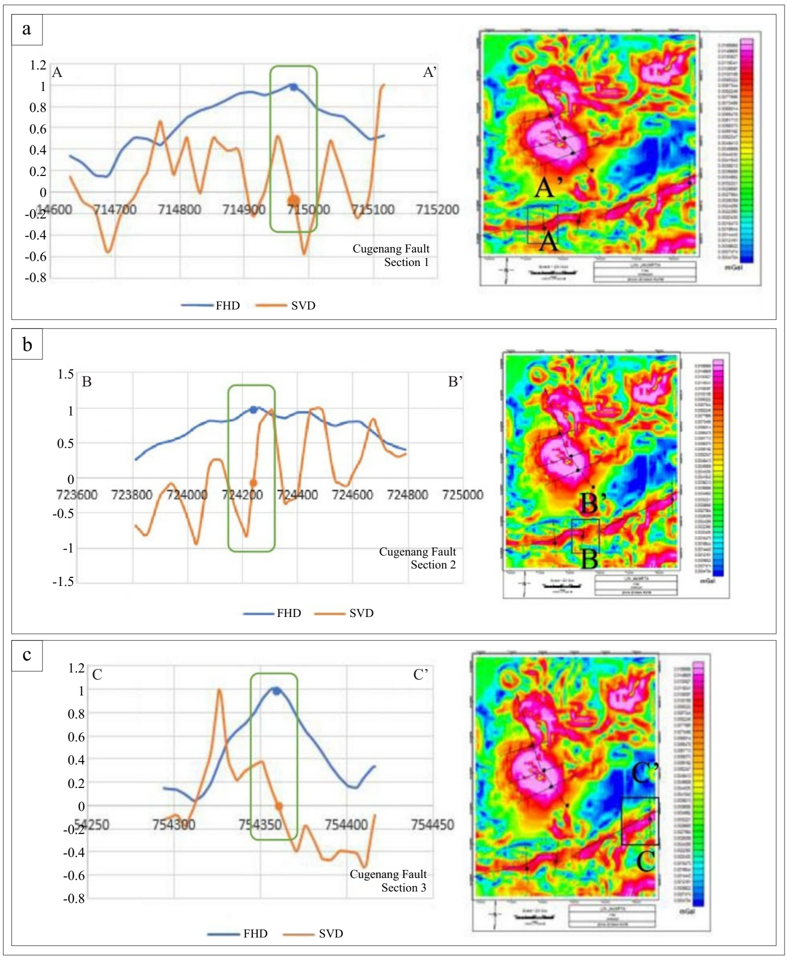

Figure 9. Slicing of FHD and SVD Gravity through Cugenang Fault (box symbol).

Table 2. Interpretation of Cimandiri Fault Type Based on Section 1 to Section 3

Cimandiri			
Fault	**SVD *max***	**SVD min**	**Type**
Slicing 1	0.5	0.5	Strike Slip Fault
Slicing 2	0.8	0.8	Strike Slip Fault
Slicing 3	0.3	0.3	Strike Slip Fault

curacies in the reading system used in relocating the hypocentre parameters of previously recorded earthquakes. The aim is to obtain a more accurate earthquake hypocentre location by applying the modified joint hypocentre determination method (Rahmaningtyas *et al*., 2020) .

In this study, earthquake relocation was carried out using Velest 3.3 software in the Cianjur area. The data used were earthquake data for the period of November 11th, 2022 - June 11th, 2023 as many as 549 and station data as many as 116 events. The data used is BMKG catalog data. The following are the results of modeling the correlation map between the gravity method and the modified joint hypocentre determination method before and after relocation. The hypocentre distribution before relocation is shown in Figure 10 where there is a vertical cross-section slice based on longitude and latitude. A series of earthquakes with latitude and longitude in the cross section were seen to form a straight line pattern that spread. The latitude cross section forms a straight line pattern in the 6.6˚ to 7˚ N-S area, while the longitude cross section forms a straight line pattern in the 106.9˚ to 107.3˚

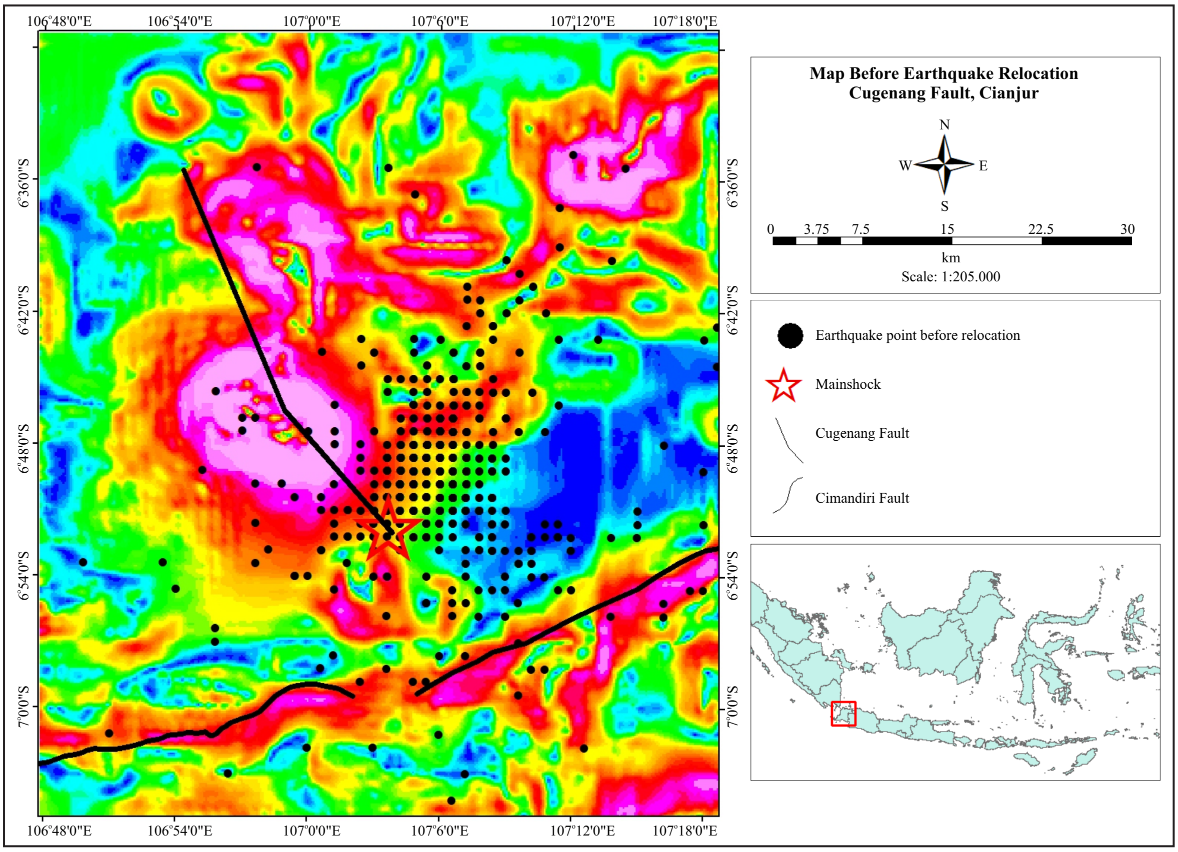

Figure 10. Map before earthquake relocation.

East area. The distribution of hypocentres is also dominated at a depth of 10 km.

The distribution of earthquakes before relocation in Figure 11 iwa seen to fill the northern part of Cianjur Regency with earthquakes spreading in the area west to southeast of Mount Gede. Most of these earthquakes were shallow earthquakes with depths of less than 40 km. The main Cianjur earthquake is marked with a red star and a series of aftershocks are marked with black circles. The figure shows the distribution of earthquake hypocentres in the Cianjur area, with the hypocentres spreading out to form boxes, not centralized or gathered in certain groups or clusters that do not show patterns corresponding to the main fault. The results after relocation show that there are certain groups or clusters that indicate high seismicity in the area. This is because the earthquake hypocentres after relocation move closer and gather to form a group on one trend of the same fault plane or structure. Trendlines or lines that show the tendency of earthquake patterns to follow the main fault structure in the region. This can indicate the presence of a cause that triggers an earthquake (Supendi *et al.*, 2022; Faridiarti, 2017).

Figure 12 shows hypocentre distribution chart modeling before relocation. Figure 13 shows that after relocation. The distribution of hypocentres is still dominated by depths of 0 to 40 km. In addition, there are several earthquake hypocentres at a depth of 10 km that form a pattern resembling a straight line. This depth is known as fixed depth, which occurs when the Seiscomp system used by BMKG automatically provides earthquake information to the public quickly. Fixed depth also occurs when the wave signals generated by an earthquake can not be clearly detected by the recording station, so Seiscomp automatically sets the depth of the earthquake at 10 km (Supendi *et al.*, 2023; Salomo *et al.*, 2015).

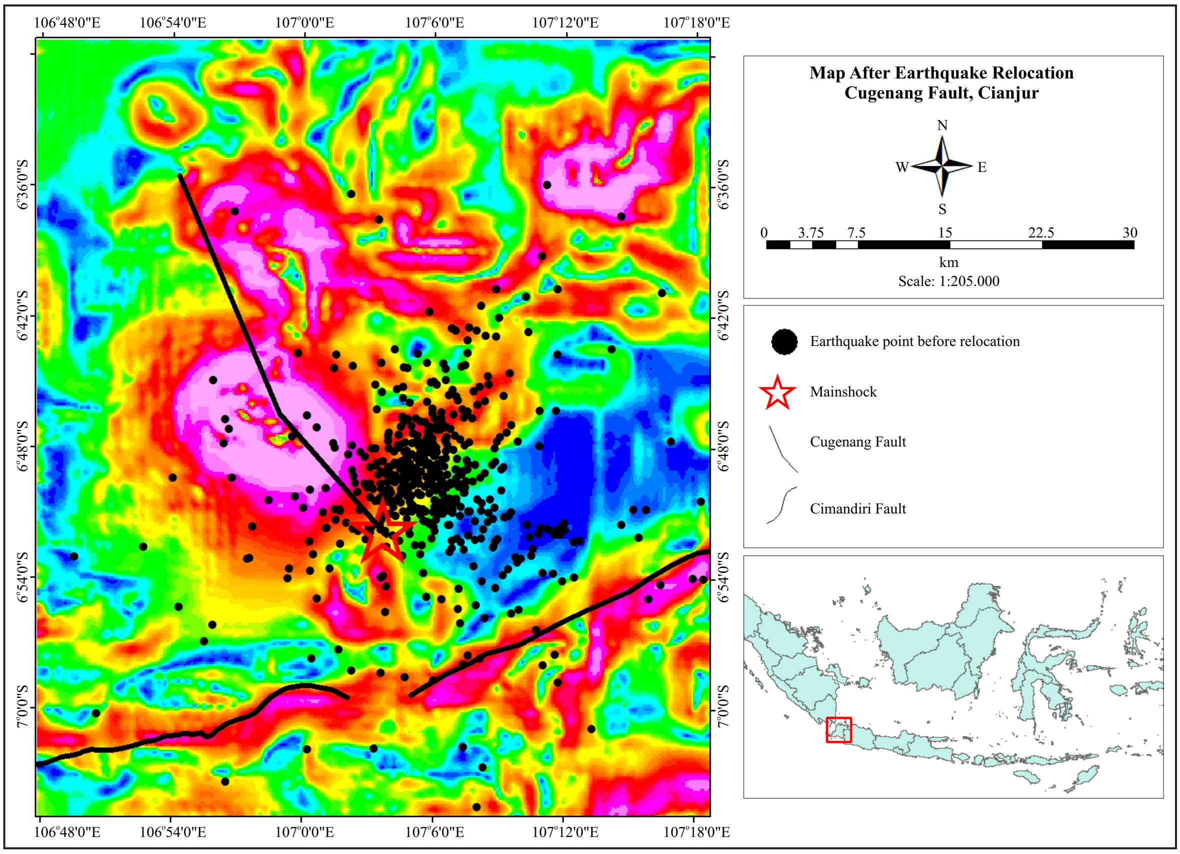

Figure 11. Map after earthquake relocation.

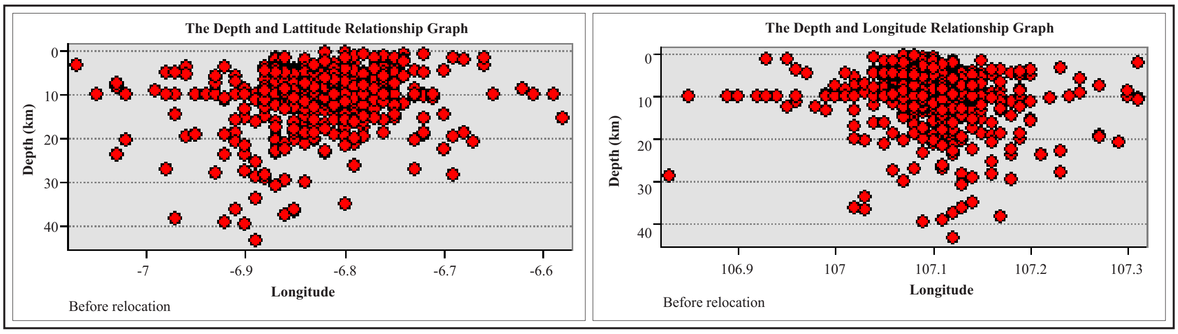

Figure 12. Hypocentre distribution chart modeling before relocation.

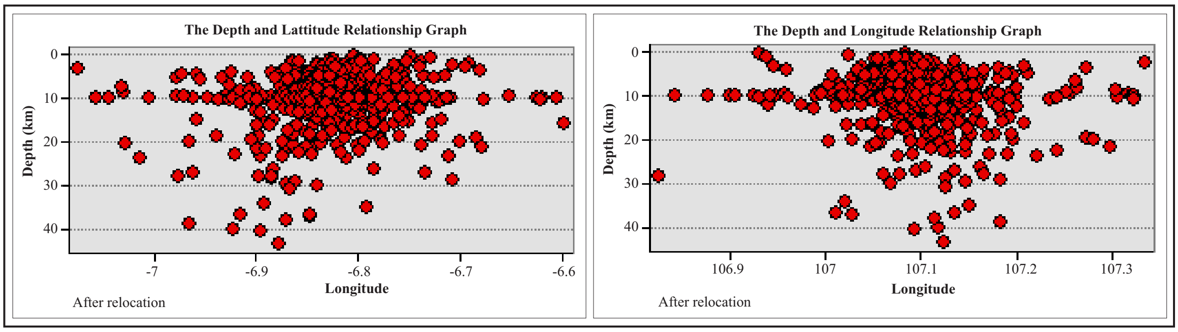

Figure 13. Hypocentre distribution chart modeling after relocation.

If observed carefully, the distribution of earthquakes after relocation gathers to form a lineation structure (straight line) with the direction of earthquake movement in Figure 13 a and b. There are two alignment structures indicated after the relocation process with the modified joint hyocentre determination method. The alignment structure is vertically along the north northeast-south southeast (NNW-SSE) northern part of Cianjur (Supendi *et al*., 2023).

The first structure in the cross section of longitude depth (longitude) was seen as an elongated alignment structure with a depth of 2 km to a depth of 25 km (Figure 13b). While the second alignment structure extends horizontally along the east northeast to west-southwest (WSW-ENE) northern part of Cianjur which is perpendicular to the first structure. The second structure is shown in the cross section of the depth of latitude (lattitude) with a depth of 2 km to a depth of 25 km (Figure 13a). The finding of this lineation is proven by the existence of tectonic activity in the Cianjur area caused by a pair of mutually perpendicular horizontal faults *(strike-slip conjugate fault)* (Supendi *et al*., 2023; Swastika *et al*., 2021).

The results of this study indicate that the 2022 Cianjur earthquake did not originate from The Cimandiri Fault, but rather from a local fault structure refered to as The Cugenang Fault. This finding is consistent with Supendi *et al*. (2023), which also shows that the earthquake epicentre was not directly associated with the Rajamandala segment of The Cimandiri Fault. Thus, The Cugenang Fault can be interpreted as a local active fault, which is likely a newly recognized structure or a reactivation of a previously under-identified fault in regional geological maps.

It should be noted that gravity-based structural interpretation has limitations due to its indirect nature in representing subsurface fault geometry. Therefore, further validation through surface geological mapping, geomorphological analysis, and integration with seismic data will be very important to strengthen these results.

Conclusions

Based on the research results, it can be concluded that:

1. Based on the FHD and SVD graph analysis, The Cugenang Fault is identified as a strike-slip fault t acted as the main source of November 21st, 2022 Cianjur earthquake. This clarifies that the earthquake did not originate from The Cimandiri Fault, but from a local structure in Cugenang.
2. The hypocentre relocation analysis using the MJHD method revealed two linear structures oriented NNE–SSE and WSW–ENE. This pattern indicates the presence of conjugate faults that are mutually perpendicular in the Cianjur area, supporting the interpretation of local tectonic activity on The Cugenang Fault.
3. This study emphasizes that gravity-based fault identification needs to be integrated with surface geological data or other geophysical methods to achieve stronger validation.
4. Future research is recommended to integrate field geological data, satellite imagery, and seismic methods to achieve more comprehensive fault mapping in Cianjur, thereby providing a better basis for future seismic hazard mitigation.

Acknowledgments

The authors would like to thank BMKG Region II and The Physics Study Programme of UIN Syarif Hidayatullah Jakarta for supporting this research.

References

Bachri, S., 2014. Pengaruh Tektonik Regional Terhadap Pola Struktur dan Tektonik Pulau Jawa. *Jurnal Geologi dan Sumberdaya Mineral*, 15 (4), p.215-221.

Faridiarti, Y.F. 2017. Relokasi Hiposenter dan Estimasi Struktur Model Kecepatan 1-D Gelombang P di Papua Menggunakan Velest 3.3. *Inovasi Fisika Indonesia*, 6 (3), p.133-139. DOI: 10.26740/ifi.v6n3.p%25p

Guci, M., Syafriani, S., and Putri, Y.T. 2020. Analysis of the mentawai region fault field based on earthquake relocation data using the modified joint hypocentre determination (MJHD) method. *Journal of Physics: Conference Series - IOP Science*, 1481 (1), p.012036. DOI: 10.1088/1742-6596/1481/1/012036.

Habibi, A.I., 2016. Relokasi Hiposenter Gempa Bumi Jawa Barat dan Sekitarnya Menggunakan Metode MJHD. *Inovasi Fisika Indonesia*, 5 (3), p.23-27

Haryanto, I., 2013. Struktur Sesar di Pulau Jawa Bagian Barat Berdasarkan Hasil Interpretasi Geologi, Bandung. *Bulletin of Scientific Contribution*, 11, p.1-10.

Jamaluddin, J., Maria, M., Ryka, H., and Afifah, R.S., 2019. Pemodelan Bawah Permukaan Bantar Karet, Jawa Barat Menggunakan Metode Gravitasi. *Jurnal Geocelebes*, 3 (2), p.59-65, DOI: 10.20956/geocelebes.v3i2.6689.

Jayatri, A.U., Multi, W., and Hayatuzzahra, S., 2023. Identifikasi Keberadaan Sesar Menggunakan Metode Gravitasi dan Analisis Second Vertical Derivative (SVD) di Bagian Selatan Kabupaten Sumbawa. *Jurnal TAMBORA*, 7 (2), p.53-57. DOI: 10.36761/jt.v7i2.2954.

Kurniasih, A., 2021. Analisis Struktur Patahan Daerah Suoh Lampung Barat Menggunakan Metode Gaya Berat dan Fault Fracture Density [Jul. 10th, 2023]. http://digilib.unila.ac.id/ id/eprint/60936.

Lubis, L.H., 2023. Teori Dasar Fisika Bumi, http://repository.uinsu.ac.id/12966/1/ Buku%20Teori%20Dasar%20Fisika%20Bumi.pdf.

Purnomo, J., Koesuma, S., and Yunianto, M., 2013. Pemisahan anomali regional-residual pada metode gravitasi menggunakan metode moving average, polynomial dan inversion. *Indonesian Journal of Applied Physics*, 3 (1), p.10.

Rahmaningtyas, N.I., Utama, W., and Lestari, W. 2020. Analisis Sumber Gempa Mikro Melalui Distribusi Lokasi Hiposenter Menggunakan Metode Double Difference Pada Lapangan Panas Bumi 'X''. *Jurnal Geosaintek*, 6 (1), p.33-42, DOI: 10.12962/j25023659.v6i1.6549.

Ronodirdjo, M.Z., 2021, Pengantar Geofisika. http://eprints.unram.ac.id/id/eprint/27348 [Jul. 10, 2023].

Saad, A.H., 2006. Understanding gravity gradients a tutorial. *The Leading Edge*, 25 (8), p.942-949, DOI: 10.1190/1.2335167.

Salomo, D., Daryono, and Subakti, H., 2015. Relocation of the 2010-2013 near the north coast of Papua earthquake sequence using Modified Joint Hypocentre Determination (MJHD) method. *AIP Conference Proceedings*, 1658 (1) p.030023. DOI: 10.1063/1.4915031.

Saria, D., Khairina, F., and Daniarsyad, G., 2020. Relokasi Hiposenter Gempa Bumi Menggunakan Metode Modified Joint Hypocentre Detremination (MJDD) Untuk Analisis Zona Subduksi Sumatra Bagian. *Jurnal Geofisika Eksplorasi*, 4 (1), p.88-104, DOI: 10.23960/jge.v4i1.9.

Soehaimi, A., 2008. Seismotektonik dan potensi kegempaan wilayah Jawa. *Indonesian Journal on Geoscience*, 3 (4), p.227-240. DOI: 10.17014/ijog.3.4.227-240

Supendi, P., Jatnika, J., Sianipar, D., and Ali, Y.H., 2022. Analisis Gempa bumi Cianjur (Jawa Barat) Mw 5. *Kelompok Kerja Sesar Aktif Dan Katalog Gempabumi Badan Meteorologi, Klimatologi, dan Geofisika (BMKG)*, p.13-16.

Supendi, P., Winder, T., Rawlinson, N., Bacon, C.A., Palgunadi, K.H., Simanjuntak, A., Kurniawan, A., Widiyantoro, S., Nugraha, A.D., Shiddiqi, H.A., Ardianto, Daryono, Adi, S.A., Karnawati, D., Priyobudi, D., Marliyani, G.I., Imran, I., and Jatnika, J., 2023. A conjugate fault revealed by the destructive Mw 5.6 (November 21, 2022) Cianjur earthquake, West Java, Indonesia. *Journal of Asian Earth Sciences,* 257, 105850, p.1-9, DOI: 10.1016/j.jseaes.2023.105830.

Swastika, D.A., Lestari, H., Astuti, A.P., Aswad, S., and Ismullah Massinai, M.F., 2021. Determination of Earthquake Hypocentre

Distribution using the Modified Joint Hypocentre Determination (MJHD) Method throughout the Palu-Koro Fault (Case Study: August-October, 2018). *IOP Conference Series: Earth and Environmental Science*, 873 (1), 012074, p1-8. DOI: 10.1088/1755-1315/873/1/012074.

Zahwa, F., Fattah, E., Hasanah, M.U., and Wijatmoko, B., 2019. Microearthquake relocation hypocentre using Modified Joint Hypocentre Determination (MJHD) method (case study: Opak fault). *IOP Conference Series: Earth and Environmental Science,* 311 (1), 012066, p.1-9. DOI: 10.1088/1755-1315/311/1/012066.